AGU PUBLICATIONS

Geophysical Research Letters

RESEARCH LETTER
10.1002/2016GL069516

Key Points:
- Slip heterogeneity of earthquakes is linked to their recurrence properties
- The quasiperiodic repeating events have persistent slip distribution
- Extremely aperiodic repeating events reveal distinct rupture characteristics

Supporting Information:
- Supporting Information S1

Correspondence to:
A. Kim,
ahyik@yokohama-cu.ac.jp

Citation:
Chen, K. H., I. Chen, and A. Kim (2016), Can slip heterogeneity be linked to earthquake recurrence?, *Geophys. Res. Lett.*, *43*, doi:10.1002/2016GL069516.

Received 9 MAY 2016
Accepted 23 JUN 2016
Accepted article online 24 JUN 2016,

Can slip heterogeneity be linked to earthquake recurrence?

Kate Huihsuan Chen[1], Iyin Chen[1], and Ahyi Kim[2]

[1]Department of Earth Sciences, National Taiwan Normal University, Taipei, Taiwan, [2]Department of Material System Sciences, Yokohama City University, Yokohama, Japan

Abstract The rupture process of two *M*4 repeating earthquake sequences in eastern Taiwan with contrasting recurrence behavior is investigated to demonstrate a link between slip heterogeneity and earthquake recurrence. The *M*3.6–3.8 quasiperiodic repeating earthquakes characterized by 3 years recurrence interval reveal overlapped slip concentrations. Inferred slip distribution for each event illustrates two asperities with peak slip of 47.7 cm and peak stress drop of 151.1 MPa. Under the influence of nearby *M*6.9 event, the *M*4.3–4.8 repeating earthquakes separated only by 6–87 min, however, reveal an aperiodic manner. There is a distinct rupture characteristic without overlap in the slip areas, suggesting that shortening of the recurrence interval by the nearby large earthquake may change the slip heterogeneity in a repeatedly ruptured asperity. We conclude that the inherent heterogeneity of stress and strength could influence the distribution of coseismic slip, which is strongly tied to the recurrence behavior.

1. Introduction

Repeating earthquake sequences (RESs) are groups of events with nearly identical waveform, location, and magnitude. They represent a repeated rupture of the same fault area. The existence of RES suggests a renewal process that takes place in the asperity surrounded by a stable sliding area. During the interseismic period, when the recurrence interval is less perturbed, the tectonic loading rate is likely the most important factor that controls the repeat time [*Chen et al*., 2007]. After a nearby large earthquake, however, the recurrence interval of repeating earthquakes (*Tr*) is dramatically shortened. The recurrence interval follows the characteristic 1/*t* decay of Omori's law as *Tr* recovers, representing accelerated fault creep along faults surrounding the rupture [*Vidale et al*., 1994; *Marone et al*., 1995; *Marone*, 1998; *Schaff et al*., 1998; *Peng et al*., 2005; *Uchida et al*., 2007; *Taira et al*., 2009]. Such behavior is similar to that of aftershocks, in which *Tr* is short immediately following the main shock and gradually increases to pre–main shock levels. Control of the recurrence interval was first explored by laboratory experiments that showed the frictional strength of the fault surface to increase with stationary contact time [*Dieterich*, 1972; *Beeler et al*., 1994; *Marone*, 1998]. Longer periods lead to higher static friction, thus a larger drop in stress. This can be observed in, for example, repeating earthquakes with the longest *Tr* tends to have a ~15% larger seismic moment (*Mo*) and possibly ~5% greater patch radius than those with shorter intervals [*Vidale et al*., 1994]. *Nadeau and McEvilly* [1999] also found that in a transient slip event during 1993 to 1998, seismic moment increased ~18% with a tenfold increase in the preceding *Tr*. However, how the change in source properties ties to recurrence behavior and how the fault strength and slip distribution respond to large earthquakes in the vicinity are not well established.

In order to address these relationships, two RESs characterized by different recurrence behaviors were selected: one is influenced by a nearby *M*6.9 earthquake, while the other is not. Using moment rate inversion, this paper aims to provide understanding of the similarities/differences in the rupture process between repeating events, to explore if slip and strength heterogeneity can be tied to recurrence behavior.

2. Data and Method

A *M*6.9 earthquake occurred in eastern Taiwan near Hualien on 19 December 2009. Following this event, a strongly accelerated rate of postseismic repeat events was observed in a RES, referred to here as Sequence A (SA), located 9 km apart. The other RES, Sequence Q (SQ) located 35 km away from the main shock, reveals a regular recurrence. Their event location, chronologies, and waveform examples are shown in Figure 1. In this paper, RES is identified by a systematic search using the composite selection criteria of *Chen et al*. [2008], which consider both waveform similarity and differential S–P times. Figures 1d and 1e show examples

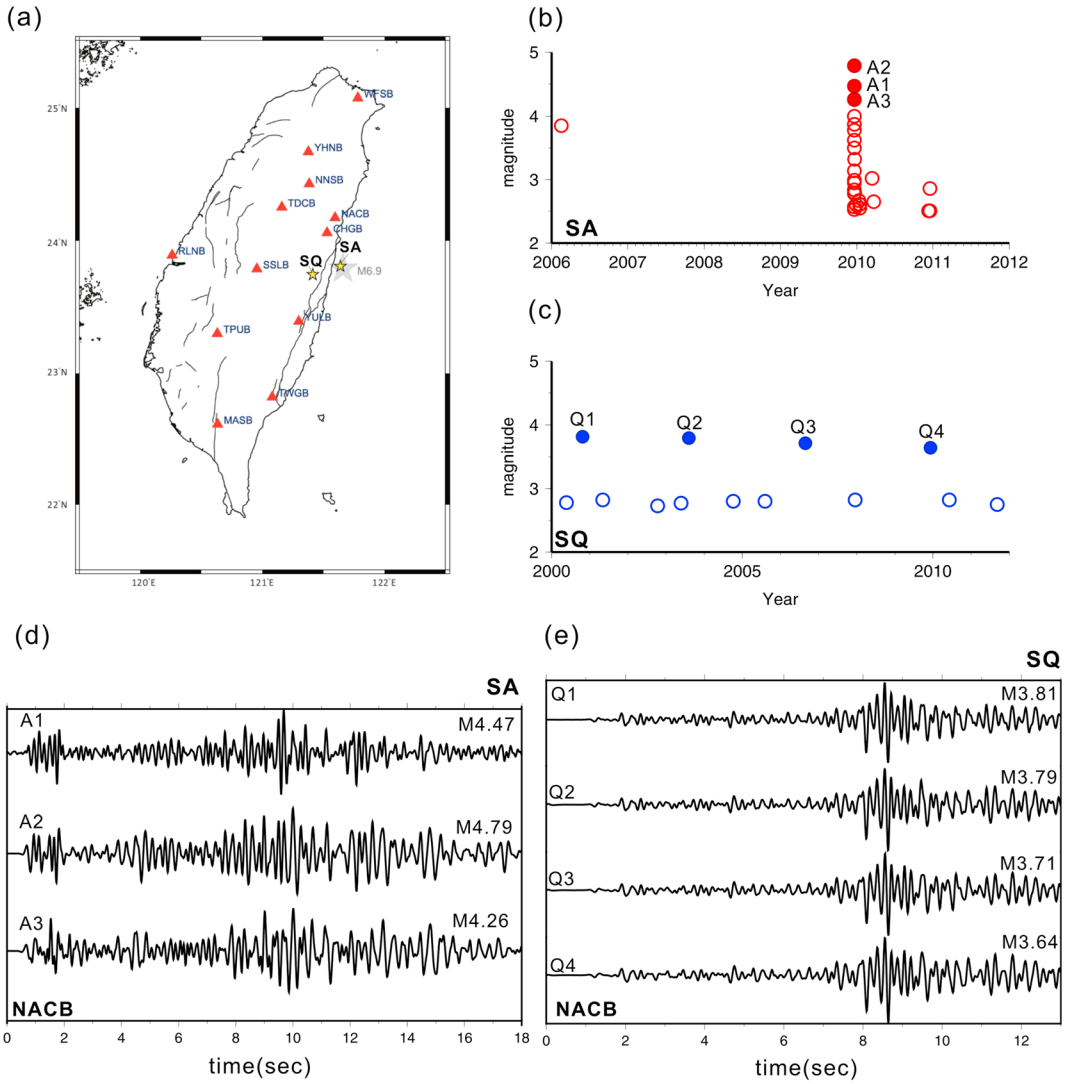

Figure 1. (a) Map of the location of seismic stations and the two repeating sequences (SA and SQ) of this study. Red triangles denote broadband seismic data by Broadband Array in Taiwan for Seismology (BATS). Yellow stars indicate the location of SA and SQ. Gray star indicates the *M*6.9 earthquake that influenced the recurrence interval of SA. (b) Event chronology for SA is denoted by filled circles, as target events considered in the slip inversion computation. Open circles indicate the events showing magnitude difference > 0.5 compared with the reference event (biggest in magnitude) in the same family. (c) Event chronology for SQ (filled circles). (d, e) The 2–8 Hz band-pass filtered, vertical component waveforms at station NACB for the repeating events in SA and SQ.

of the 2–8 Hz band-pass-filtered waveforms for SA and SQ at the NACB station. Figure S1 (supporting information) shows the colocation of repeating events using precise relocation by the hypoDD [*Waldhauser*, 2001] and *Vp*/*Vs* methods [*Chen et al*., 2008], assuming a circular rupture with 3 MPa stress drop. Note that identification scheme adopted here requires a similar magnitude range (magnitude difference < 0.5), given the assumption that repeating events rerupture the same fault patch. Therefore, the repeating earthquakes family may be comprised of multiple repeating sequences. The SQ and SA studied here are denoted by filled circles in Figures 1b and 1c, while open circles indicate the repeating events in the same family.

As shown in Figure 1b, SA family has a varying magnitude in the *M*2.5–4.8 range, while the number of events increases to 15 on the day of the main shock and gradually decreases with time. Like the postseismic variation of *Tr* observed in other study areas [e.g., *Schaff et al*., 1998; *Nadeau and McEvilly*, 1999; *Peng et al*., 2005; *Uchida et al*., 2007, 2009; *Chen et al*., 2010b; *Uchida et al*., 2015], the accelerated recurrence of SA may reflect an increase in loading rate by coseismic stress changes from the main shock rupture. As shown in Figure 1c,

Table 1. Repeating Earthquake Sequence Parameters Used in This Study

Sequence	ID	Date	Time (UTC)	Latitude	Longitude	Depth (km)	M_L	VR (%)	Peak/Average Slip (cm)	Peak/Average Stress Drop (Mpa)
A	A1	2009/12/19	14:09:07	23.8550	121.634	40.32	4.47	94.922	65.54/13.14	89.27/8.36
	A2	2009/12/19	14:13:51	23.8155	121.663	40.62	4.79	94.573	113.19/22.27	114.47/13.1
	A3	2009/12/19	15:41:21	23.8227	121.659	40.19	4.26	94.997	41.52/10.47	52.95/6.74
	eGF1	2009/12/19	14:50:18	23.8292	121.659	40.20	3.50			
Q	Q1	2000/10/22	17:25:25	23.7212	121.469	16.69	3.81	94.338	47.69/13.49	147.63/19.11
	Q2	2003/08/06	18:01:37	23.7335	121.437	18.44	3.79	93.512	41.59/7.96	155.11/14.45
	Q3	2006/08/26	01:51:44	23.7333	121.404	19.43	3.71	94.104	33.95/9.14	111.52/14.26
	Q4	2009/12/07	06:05:28	23.7407	121.405	20.12	3.64	90.617	18.24/5.04	64.36/8.96
	eGF2	2001/05/04	17:46:07	23.7290	121.439	16.20	2.82			

The SQ family has dominant magnitudes of *M*2.8 and *M*3.8 with repeat times of 1.4 and 3.0 years, respectively. The coefficient of variation in *Tr* is 0.45 and 0.06 for the groups of *M*2.8 and *M*3.8 repeating events, respectively, indicating quasiperiodicity of recurrence for both magnitude levels.

To study how the change in source properties ties to recurrence behavior, empirical Green's function (eGf) deconvolution is conducted to extract the relative source time function (RSTF) for a target event. The obtained RSTF is later introduced in kinematic source inversion modeling of slip distribution in an asperity [e.g., *Mori and Hartzell*, 1990; *Mori*, 1993; *Dreger*, 1994; *Hough and Dreger*, 1995; *Dreger et al*., 2007]. A detailed description of methodology can be found in *Hough and Dreger* [1995] and is also described in the supporting information.

In this study, the highest magnitudes in the two sequences were selected as the target events: *M*3.8 for SQ family and *M*4.5 for SA family, as shown with filled circles in Figures 1b and 1c. The parameters of selected target events and eGfs for both sequences are listed in Table 1. The selection of eGfs requires highly similar waveforms at more than five stations with a variety of azimuths when paired with each target event. Given that the repeating events are located near the edge of the Broadband Array in Taiwan for Seismology (BATS) seismic network with relatively few stations present before 2003, only one eGf meets such requirements for SQ and SA. With three component 100 Hz sampled velocity records from BATS, RSTF was obtained at each station using Landweber deconvolution (PLD) [*Bertero*, 1989]. To remove low-frequency noises, the data were high pass filtered with a cutoff frequency of 0.5 Hz. The detailed procedure of the deconvolution is shown in the supporting information.

Figure 2 shows an example of vertical component waveforms, the RSTF, and the comparable observed and synthetic waveforms at different stations for the *M*3.8 target event and *M*2.8 eGf in SQ (example for SA is shown in Figure S2). In each inversion the rupture velocity, rise time, and smoothing factor were selected to meet the maximum variation reduction or residual sum of square (see Figures S3 and S4 and Table S1 for details).

3. Slip Features for Quasiperiodic and Aperiodic Sequences

Slip inversion result for four target events in SQ and three target events in SA with corresponding goodness of fit between the observed and synthetic RSTFs are shown in Figure 3. The uncertainty of slip can be addressed by the coefficient of variation (standard deviation divided by the mean) in slip (COV_{slip}) using a Jackknife resampling method [*Hartzell et al*., 2007] that systematically leaves out each station at a time for different measures of slip. Lower COV_{slip} represents smaller uncertainly in fault slip.

The 2000, 2003, 2006, and 2009 *M*3.8 repeating events in SQ reveal two slip concentrations with maximum slips of 47.7 cm, 41.6 cm, 34.0 cm, and 18.2 cm, respectively. The areas experiencing major slip (i.e., 50% of maximum slip) are located within the area with small COV_{slip} ($<$0.4, denoted by gray line in Figure S5), which reveal two reliable asperities for each event. The overall slip distribution is similar among four events: the major asperity occurs downdip from the projected hypocenter, while the secondary asperity is located near the hypocenter with smaller slip (Figures 3a–3d). When the relocated relative position of the SQ event is plotted in plan view, it can be observed that the detailed feature applied to the earthquake relocation reveals significant overlap with slightly different feature (Figure 3h).

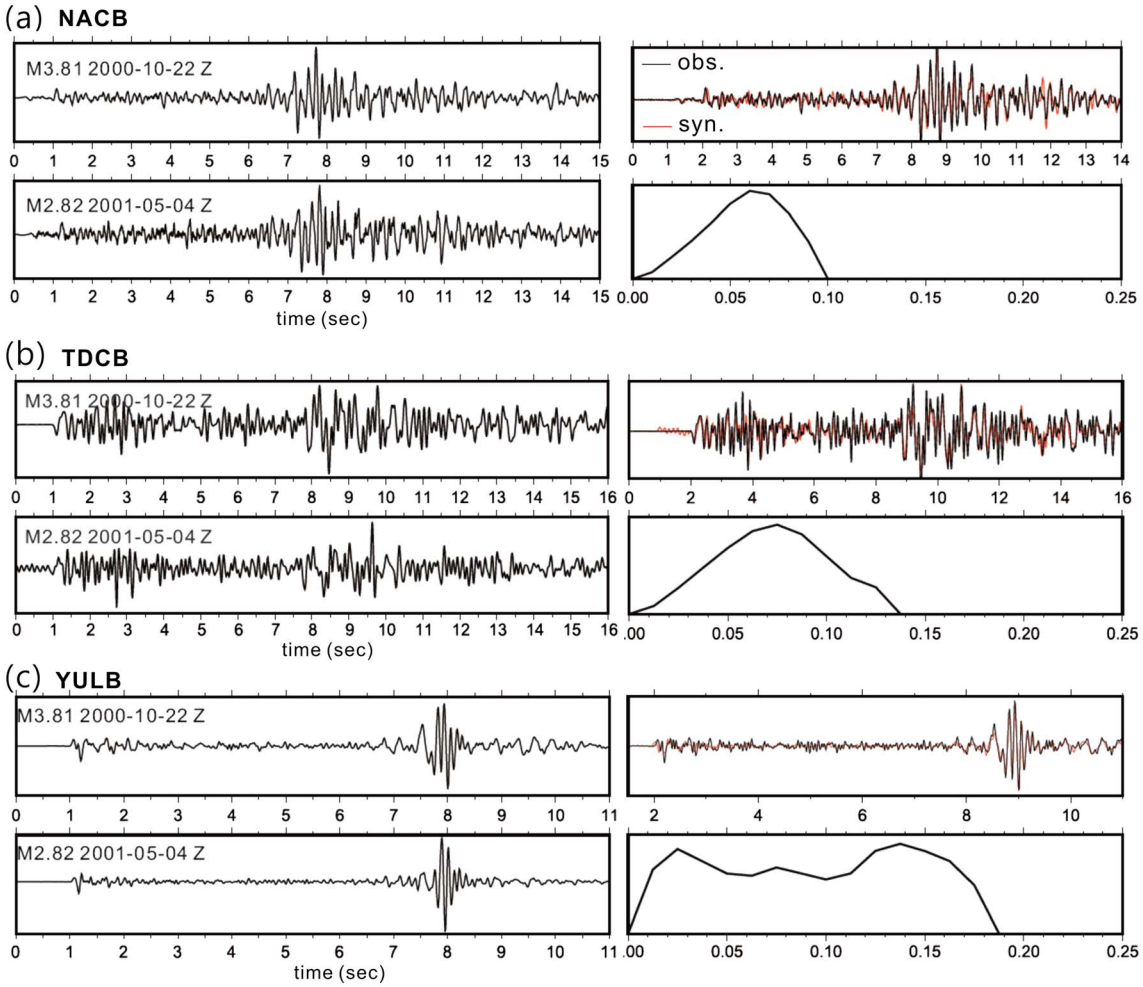

Figure 2. Waveforms and relative source time functions between the target event and eGf for SQ at stations (a) NACB, (b) TDCB, and (c) YULB. Figures 2a–2c (left) show vertical component waveforms for the first target event and eGf event in sequence SQ. Waveforms are 0.5 Hz high-pass filtered. Figures 2a–2c (right) show comparisons between the observed waveform (black) and synthetic waveform (red) derived from deconvolution using eGf and the RSTF.

Figures 3e–3g show slip distribution of *M*4.5 repeating events in sequence SA. The maximum slip for the first *M*4.8 event (A2) is 113.2 cm, significantly higher than 65.5 cm and 41.5 cm from the other two *M*4.5 (A1) and *M*4.3 (A3) events. Among the three repeating events, the area experiencing major slip is around the epicenter within a similar spatial range. However, when the relocated position is applied, a very limited overlap exists between the slip areas among *M*4.5 events (Figure 3i). The distinct rupture characteristics for these repeating events indicate a possible shielding effect (i.e., stress shadow region) [*Johnson*, 2010] from the previous rupture. When comparing with a wide range of event magnitudes from other repeating event studies [*Park and Mori*, 2007; *Uchida et al*., 2015; *Kim et al*., 2016], we find that the average slip appears to be a function of earthquake magnitude, while the peak slip does not show such a strong linear correlation (Figure 4). This may indicate that the main controlling factor(s) for average and peak slip is different.

The coseismic stress change can be determined later using the method proposed by *Ripperger and Mai* [2004]. This method converts slip to stress change in each modeled subfault. The spatial concentration of stress drop is found to be consistent with the areas showing maximum slip, while the peak value is also similar among events in a common sequence. SQ reveals peak stress drop in the 64.4–155.1 MPa range with an average stress drop of 8.9 to 19.1 MPa. By contrast, SA reveals peak stress drop in the 52.9–114.5 MPa range with an average of 6.7–13.1 MPa. The measurements of peak stress drop are in a similar range to that inferred for *M*2 repeating earthquakes at Parkfield [*Dreger et al*., 2007], indicating relatively isolated fault areas capable of developing large stress concentration over time.

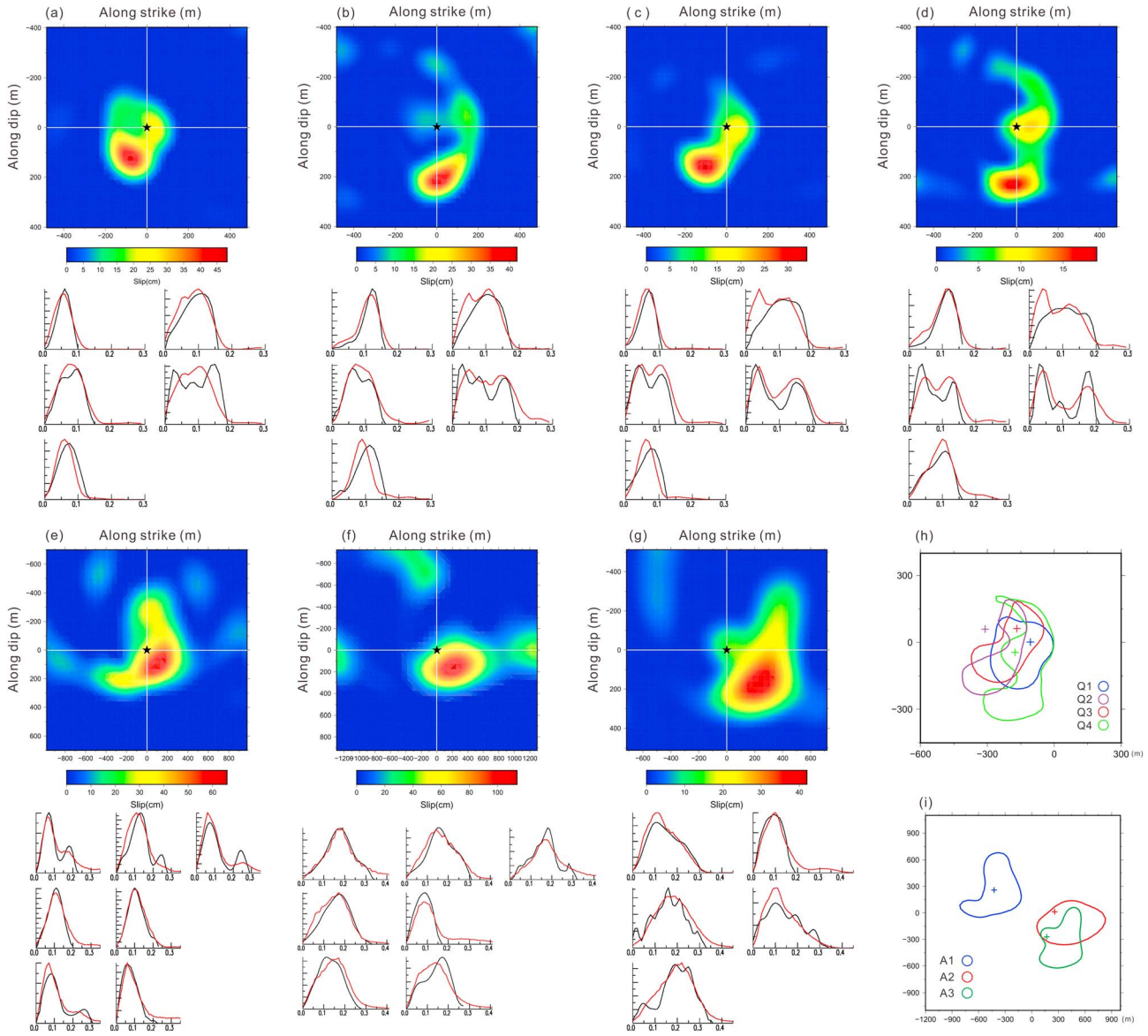

Figure 3. (a–d) *M*3.8 target repeating events in SQ and (e–g) *M*4.5 target repeating events in SA. Figures 3a–3g (top) show slip distribution of the *M*3.8 target repeating events and Figures 3a–3g (bottom) show the observed (black) and synthetic (red) relative source time functions. Superimposed slip areas are shown in Figures 3h and 3i; they are defined by 20% of the maximum slip for all target events for SQ and SA, respectively.

4. Response of Rupture Process to Large Earthquake

After the 2011 *M*9.0 Tohoku earthquake, a *M*4.8 RES in Kamaish revealed a dramatic change in magnitude and recurrence interval. For the first post-Tohoku repeating event, the recurrence interval decreased from 5.5 years to 9 days, while the magnitude increased from *M*4.8 to *M*5.9. Such synchronized phenomena suggest a similar mechanism responsible for the increase in magnitude and decrease in repeat time. One year after the Tohoku event, the magnitude returned to the original level but the recurrence interval (0.6 years) was still shorter than the pre-Tohoku value (5.5 years). *Uchida et al*. [2013] proposed that a switch in slip mode, from aseismic to seismic, is needed to explain the expanding slip area for post-Tohoku repeating events. Such mode-changing behavior took place in a seismic-to-aseismic transition zone, a conditionally stable area where slip behavior changes with loading rate. At low loading rates, the conditionally stable area is generally an aseismic slip region, but when the loading rate increases, this area experiences seismic slip.

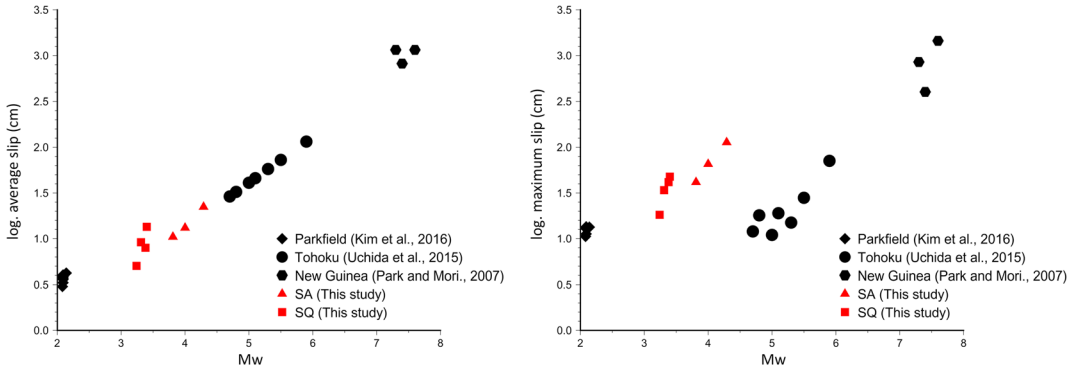

Figure 4. (a) Average slip and (b) peak slip as a function of event magnitude for repeating earthquakes from different studies. Different symbols indicate measurements from different areas as shown in the figure key.

After a large earthquake, the shortened recurrence interval in RES is not always accompanied by a magnitude change. Following the 2004 *M*6 Parkfield event, most RES experienced an immediate increase in seismic moment and subsequent decay as recurrence interval returned to the pre-Parkfield level. However, RES with the larger magnitude ($M \sim 2$) reveals very small variations in seismic moment [*Chen et al*., 2010b]. Using RSTF waveform inversion, *Kim et al*. [2016] examined eight post-Parkfield repeating events in this sequence that began 2 days after the main shock. The slip inversion revealed a spatially stable rupture area and constant average slip for all events, while a significant peak slip reduction (13.5 to 10.5 cm) and corresponding stress drop reduction (94.7 to 69.5 MPa) was observed in the post-Parkfield events. These authors concluded that the postseismic $M \sim 2$ repeating events revealed a change in strength but not magnitude, likely associated with the healing process in the same asperity.

In this present study, the three SA repeating events that occurred shortly after the 2009 *M*6.9 event are only separated by several minutes to a few hours. They have various peak slip values (41.5–113.2 cm) with different slip distribution concentrations. Unlike the consistent rupture areas in RES after the *M*9.0 Tokohu and Parkfield *M*6.0 events, the superimposition of major slip areas in Figure 3i shows nonoverlapped ruptures for repeating events in SA. The very short repeat time for the post main shock repeating events (6 min and 87 min) suggests that a shielding effect from previous ruptures is involved. It may take longer than a few days to recover enough strength to allow for rerupture to be possible in the same asperity. One may argue that in SA family, the pre-M6.9 repeating event that occurred in 2006 provides more information for rupture characteristics during interseismic period. This event, however, has (1) much smaller magnitude (*M*3.8) than the average magnitude of the selected SA target events (*M*4.5) and (2) similar magnitude to the eGf (*M*3.5), leading to a bad condition for reliable eGf analysis.

5. Response of Recurrence Interval, Magnitude, Strength, and Slip Heterogeneity to Large Earthquake

Recurrence interval, magnitude, strength, and slip heterogeneity of the repeating events appear to respond differently to a nearby main shock. The recurrence interval is strongly controlled by the accelerated loading rate surrounding the rupture [e.g., *Nadeau and McEvilly*, 1999; *Peng et al*., 2005; *Taira et al*., 2009; *Chen et al*., 2010b; *Uchida et al*., 2015]. Such influence is demonstrated not only for *M*6–9 main shocks [*Vidale et al*., 1994; *Marone et al*., 1995; *Schaff and Beroza*, 2004; *Peng et al*., 2005; *Templeton et al*., 2009; *Uchida et al*., 2004, 2015] but also *M*4–5 events [*Chen et al*., 2010a], suggesting that the recurrence interval is very sensitive to the accelerated loading rate induced by the main shock. The degree of triggering effect, if defined by RES's regularity and time difference between repeating events and nearby main shocks, is likely controlled by the size of main shock and the distance from the main shock [*Chen et al*., 2013].

Postseismic magnitude variation is likely controlled by the frictional property of the asperity that changes significantly with loading rate. If repeating earthquakes can be described by rupture of isolated velocity-weakening asperities surrounded by velocity-strengthening fault areas, *Chen et al*. [2010b] noted that as loading velocity varies, the degree to which slip is accommodated aseismically is different for different

asperity radii and nucleation size. A small asperity may have a small fraction of its slip accumulated seismically; therefore, it can grow in size when experiencing higher loading rate. This is similar to the interpretation of post-Tohoku repeating events by *Uchida et al*. [2015], as we addressed earlier in section 4. After the *M*9.0 Tohoku earthquake, most of the magnitude increase occurred in areas of higher postseismic slip [*Uchida et al*., 2015]. After the *M*6.0 Parkfield event, however, most of the large magnitude variation occurred in a smaller asperity characterized by greater aseismic slip area compared with the larger asperity [*Chen et al*., 2010b]. *Peng et al*. [2005] demonstrated a depth-dependent relationship between seismic moment and recurrence interval, which is also a result of dependency on loading rate. How the magnitude of postseismic slip, fault zone rheology and frictional properties inside the asperity influence magnitude variation requires additional collection of repeating event data associated with different main shocks for further study.

The strength of the asperity, if inferred from maximum slip and peak stress drop, is generally a function of its own magnitude. Slip inversion on repeating sequences from different study areas [*Park and Mori*, 2007; *Uchida et al*., 2015; *Kim et al*., 2016] reveals the peak slip that is not in linear proportion to the moment magnitude (Figure 4b), unlike average slip in Figure 4a. With a general trend of magnitude dependency visible for each area in Figure 4b, we argue that other than magnitude, smaller asperity have stronger strength. This supports the interpretation of weak dependency of recurrence interval on seismic moment revealed from worldwide repeating earthquakes in *Chen et al*. [2007]. Peak slip occurs where the seismic moment is allowed to accumulate over time. In this study, the slip concentrations did not occur at the same spot within a few hours of the main shock. This could be explained by the halt of coseismic slip (stress shadow) from the previous rupture. We infer that slip heterogeneity, as a result of heterogeneous stress accumulation on a fault, relies on the stress condition in each subarea of the fault plane, whereas stress condition inside the asperity controls where the peak slip takes place. This could be tested using a greater range of magnitude for slip inversion in the future and has potential application in monitoring the temporal evolution of stress state and fault strength.

6. Conclusion

The source properties of two RES characterized by different responses to a nearby *M*6.9 earthquake have been studied in terms of recurrence behavior. The quasiperiodic sequence (SQ) is characterized by a recurrence interval of ~3 years, while SA is an aperiodic sequence accelerated at the time of a *M*6.9 earthquake in the immediate vicinity. By inverting seismic moment rate functions obtained from empirical Green's function deconvolution, the slip distribution of repeating events in the two different sequences was compared.

In SQ, the four different ruptures reveal significant overlap and a good consistency in overall characteristics. In SA, the three events that were separated from the main shock by 6–87 min reveal distinct rupture characteristics and do not overlap, suggesting that a time span greater than a few hours is needed, to recover the strength on the fault sufficiently to allow the rerupture to occur in the same asperity.

The results of this study also show that the inherent heterogeneity of stress and strength is strongly tied to the irregularity of earthquake recurrence; the slip heterogeneity reflects the heterogeneous stress accumulated on a fault, which therefore can be regarded as an indicator of temporal change in the stress state and fault strength.

Acknowledgments

We thank Wen-Tzong Liang for helpful discussions. Seismic data were obtained from the archives at the Broadband Array in Taiwan for Seismology (BATS) operated by Institute of Earth Sciences, Academia Sinica in Taiwan. Figures were made with GMT [*Wessel and Smith*, 1995]. This work was supported by Taiwan MOST grant 103-2116-M-003-001-MY5. This work was also partially supported by grants from the Japan Society for the Promotion of Science KAKENHI grant 25870600.

References

Beeler, N. M., T. E. Tullis, and J. D. Weeks (1994), The roles of time and displacement in the evolution effect in rock friction, *Geophys. Res. Lett.*, *21*, 1987–1990, doi:10.1029/94GL01599.

Bertero, M. (1989), Linear inverse and ill-posed problems, in *Advances in Electronics and Electron Physics*, vol. 75, pp. 1–120, Academic, New York.

Chen, K. H., R. M. Nadeau, and R. J. Rau (2007), Towards a universal rule on the recurrence interval scaling of repeating earthquakes?, *Geophys. Res. Lett.*, *34*, L16308, doi:10.1029/2007GL030554.

Chen, K. H., R. M. Nadeau, and R. J. Rau (2008), Characteristic repeating earthquakes in an arc-continent collision boundary zone—The Chihshang fault of eastern Taiwan, *Earth Planet. Sci. Lett.*, *276*, 262–272, doi:10.1016/j.epsl.2008.09.021.

Chen, K. H., R. Bürgmann, and R. M. Nadeau (2010a), Triggering effect of M 4–5 earthquakes on the earthquake cycle of repeating events at Parkfield, *Bull. Seismol. Soc. Am.*, *100*(2), 522–531, doi:10.1785/0120080369.

Chen, K. H., R. Bürgmann, R. M. Nadeau, T. Chen, and N. Lapusta (2010b), Postseismic variations in seismic moment and recurrence interval of repeating earthquakes, *Earth Planet. Sci. Lett.*, *299*, 118–125, doi:10.1016/j.epsl.2010.08.027.

Chen, K. H., R. Burgmann, and R. M. Nadeau (2013), Do earthquakes talk to each other? Triggering and interaction of repeating sequences at Parkfield, *J. Geophys. Res. Solid Earth*, *118*, 165–182, doi:10.1029/2012JB009486.

Dieterich, J. H. (1972), Time-dependent friction in rocks, *J. Geophys. Res.*, *77*, 3690–3697, doi:10.1029/JB077i020p03690.
Dreger, D. (1994), Empirical Green's function study of the January 17, 1994 Northridge mainshock (Mw6.7), *Geophys. Res. Lett.*, *21*, 2633–2636, doi:10.1029/94GL02661.
Dreger, D., R. M. Nadeau, and A. Chung (2007), Repeating earthquake finite source models: Strong asperities revealed on the San Andreas Fault, *Geophys. Res. Lett.*, *34*, L23302, doi:10.1029/2007GL031353.
Hartzell, S. H., P. Liu, C. Mendoza, J. Chen, and K. M. Larson (2007), Stability and uncertainty of finite-fault slip inversions: Application to the 2004 Parkfield, California, earthquake, *Bull. Seismol. Soc. Am.*, *97*, 1911–1934, doi:10.1785/0120070080.
Hough, S. E., and D. Dreger (1995), Source parameters of the 23 April 1992 M6.1 Joshua Tree, California, earthquake and its aftershocks: Empirical Green's function analysis of GEOS and TERRAscope data, *Bull. Seismol. Soc. Am.*, *85*, 1576–1590.
Johnson, L. R. (2010), An earthquake model with interacting asperities, *Geophys. J. Int.*, *182*, 1339–1373.
Kim, A., D. S. Dreger, T. Taira, and R. M. Nadeau (2016), Changes in repeating earthquake slip behavior following the 2004 Parkfield mainshock from waveform empirical Green's functions finite-source inversion, *J. Geophys. Res. Solid Earth*, *121*, 1910–1926, doi:10.1002/2015JB012562.
Marone, C. (1998), Laboratory-derived friction laws and their application to seismic faulting, *Annu. Rev. Earth Planet. Sci.*, *26*, 643–696.
Marone, C., J. E. Vidale, and W. L. Ellsworth (1995), Fault healing inferred from time dependent variations in source properties of repeating earthquakes, *Geophys. Res. Lett.*, *22*, 3095–3098, doi:10.1029/95GL03076.
Mori, J. (1993), Fault plane determinations for three small earthquakes along the San Jacinto Fault, California: Search for cross faults, *J. Geophys. Res.*, *98*, 17,711–17,722, doi:10.1029/93JB01229.
Mori, J., and S. Hartzell (1990), Source inversion of the 1988 Upland earthquake: Determination of a fault plane for a small event, *Bull. Seismol. Soc. Am.*, *80*, 507–518.
Nadeau, R. M., and T. V. McEvilly (1999), Fault slip rates at depth from recurrence intervals of repeating microearthquakes, *Science*, *285*(5428), 718–721.
Park, S. C., and J. Mori (2007), Are asperity patterns persistent? Implication from large earthquakes in Papua New Guinea, *J. Geophys. Res.*, *112*, B03303, doi:10.1029/2006JB004481.
Peng, Z., J. E. Vidale, C. Marone, and A. Rubin (2005), Systematic variations in recurrence interval and moment of repeating aftershocks, *Geophys. Res. Lett.*, *32*, L15301, doi:10.1029/2005GL022626.
Ripperger, J., and P. M. Mai (2004), Fast computation of static stress changes on 2D faults from final slip distributions, *Geophys. Res. Lett.*, *31*, L18610, doi:10.1029/2004GL020594.
Schaff, D. P., and G. C. Beroza (2004), Coseismic and postseismic velocity changes measured by repeating earthquakes, *J. Geophys. Res.*, *109*, B10302, doi:10.1029/2004JB003011.
Schaff, D. P., G. C. Beroza, and B. E. Shaw (1998), Postseismic response of repeating aftershocks, *Geophys. Res. Lett.*, *25*, 4549–4552, doi:10.1029/1998GL900192.
Taira, T., P. G. Silver, F. Niu, and R. M. Nadeau (2009), Remote triggering of fault-strength changes on the San Andreas fault at Parkfield, *Nature*, *461*, 636–639, doi:10.1038/nature08395.
Templeton, D. C., R. M. Nadeau, and R. Bürgmann (2009), Distribution of postseismic slip on the Calaveras fault, California, following the 1984 M6. 2 Morgan Hill earthquake, *Earth Planet. Sci. Lett.*, *277*(1–2), 1–8.
Uchida, N., A. Hasegawa, T. Matsuzawa, and T. Igarashi (2004), Pre- and post-seismic slip on the plate boundary off Sanriku, NE Japan associated with three interpolate earthquakes as estimated from small repeating earthquake data, *Tectonophysics*, *385*, 1–15.
Uchida, N., T. Matsuzawa, W. L. Ellsworth, K. Imanishi, T. Okada, and A. Hasegawa (2007), Source parameters of a M4.8 and its accompanying repeating earthquakes off Kamaishi, NE Japan: Implications for the hierarchical structure of asperities and earthquake cycle, *Geophys. Res. Lett.*, *34*, L20313, doi:10.1029/2007GL031263.
Uchida, N., S. Yui, S. Miura, T. Matsuzawa, A. Hasegawa, Y. Motoya, and M. Kasahara (2009), Quasi-static slip on the plate boundary associated with the 2003 M8.0 Tokachi-oki and 2004 M7.1 off-Kushiro earthquakes, Japan, *Gondwana Res.*, *16*, 527–533.
Uchida, N., K. Shimamura, T. Matsuzawa, and T. Okada (2015), Postseismic response of repeating earthquakes around the 2011 Tohoku-oki earthquake: Moment increases due to the fast loading rate, *J. Geophys. Res. Solid Earth*, *120*, 259–274, doi:10.1002/2013JB010933.
Vidale, J. E., W. L. Ellsworth, A. Cole, and C. Marone (1994), Variations in rupture process with recurrence interval in a repeated small earthquake, *Nature*, *368*, 624–626.
Waldhauser, F. (2001), HypoDD – a program to compute double-difference hypocenter locations, *U. S. Geol. Surv. Open File Rep.*, 1-113.
Wessel, P., and W. H. F. Smith (1995), New version of the Generic Mapping Tools released, *Eos Trans., AGU*, *76*, 329.